journal

J. Am. Ceram. Soc., 97 [10] 3052–3061 (2014)
DOI: 10.1111/jace.13124

Synthetic Aragonite ($CaCO_3$) as a Potential Additive in Calcium Phosphate Cements: Evaluation in Tris-Free SBF at 37°C

Jin H. Lee,[‡] Andrew S. Madden,[§] Waltraud M. Kriven,[‡,*] and A. Cuneyt Tas[‡,†,*]

[‡]Department of Materials Science and Engineering, University of Illinois at Urbana-Champaign, Urbana, IL 61801

[§]School of Geology and Geophysics, University of Oklahoma, Norman, OK 73019

Conventional SBF (simulated/synthetic body fluid) solutions are buffered at pH 7.4°C and 37°C using 50 mM Tris [$(HOCH_2)_3CNH_2$]. Tris is not present in human blood or metabolism and its high concentration makes it the third major component of SBF solutions. All three crystalline polymorphs of calcium carbonate (calcite, aragonite and vaterite) have never been tested simultaneously in an SBF solution. This study presents the SBF-testing of the particles of these polymorphs at 37°C in Na-*L*-lactate (22 mM)-buffered *Lac*-SBF solution. While the calcite rhombohedra remained completely inert in the solution, vaterite spherulites and aragonite needles accrued apatitic CaP (calcium phosphate) deposits on their surfaces. Mg-doped (1050 ppm) synthetic aragonite particles did not transform into calcite for 96 h in the *Lac*-SBF solution while increasing their BET surface area by about 560% via the apatitic CaP deposits. Given the well-established use of calcite powders in CaP cement formulations, synthetic aragonite particles may be a potential replacement for calcite due to their rapid response to blood plasma-like solutions in between 24 and 48 h at 37°C.

I. Introduction

$CaCO_3$ (calcium carbonate) is an important material of marine biomineralization and geological formations (e.g., stalactites and stalagmites).[1–3] Calcium carbonate can be synthetically produced by aqueous precipitation processes in one of the three anhydrous polymorphs; calcite, aragonite and vaterite. X-ray-amorphous calcium carbonate (ACC) can be synthesized at room temperature as a precursor phase in calcite or vaterite syntheses.[4] Calcium carbonate monohydrate (*monohydrocalcite*) and calcium carbonate hexahydrate (*ikaite*) may be regarded as naturally occurring hydrous polymorphs of $CaCO_3$ and both are stable at temperatures below 10°C prior to their transformation into calcite.[5] At room temperature and pressure, calcite is the most stable and abundant polymorph of calcium carbonate, while vaterite (μ-$CaCO_3$), named after Heinrich Vater,[6] is known to be the least stable among the anhydrous polymorphs. Synthetic $CaCO_3$ powders, usually of the calcite form, are widely used in cosmetics, food, toothpaste, plastic, paper making, ink, paint, textile, pharmaceutical, and rubber industries.

Calcium phosphate cement (CPC) pastes provide surgeons with the ability to fill bone voids with a biocompatible and malleable material mimicking (upon setting) the mineral of bones.[7] The mineral of bones is a carbonated (5.8 wt% CO_3) and ionically substituted (0.7% Na^+, 0.55% Mg^{2+} and 0.03% K^+) apatite-like (apatitic) calcium phosphate (CaP).[8] CPCs usually contain either α-tricalcium phosphate [α-TCP: α-$Ca_3(PO_4)_2$] or tetracalcium phosphate [TTCP: $Ca_4(PO_4)_2O$], or both, in their powder components. The very first calcium phosphate cement paste, containing α-TCP, was patented in 1974 by Driskell *et al.*[9] α-TCP and TTCP powders, in their pure forms, both undergo rapid *in situ* hydrolysis into cryptocrystalline, Ca- and OH-deficient (CDHA, *calcium-deficient hydroxyapatite*: $Ca_9(HPO_4)(PO_4)_5OH$), upon kneading with an aqueous setting solution.[10–16] The compositions of the commercialized CPCs have been tabulated by Bohner *et al.*[17]

To simultaneously decrease the setting time of pure α-TCP[13] or TTCP[14,18] from about an hour to the vicinity of 9–14 min and to further increase the compressive and tensile strength of the set cements, CPC developers [e.g., for Norian SRS® (DePuy Synthes, West Chester, PA), Calcibon® (Biomet Deutschland GmbH, Berlin, Germany), Biopex® (Mitsubishi Materials Corporation, Tokyo, Japan), Rebone® (Shanghai Rebone Biomaterials Co., Shanghai, China) cements] usually added $CaCO_3$ (always in calcite form), MCPM [monocalcium phosphate monohydrate, $Ca(H_2PO_4)_2{\cdot}H_2O$], DCPD (dicalcium phosphate dihydrate, brushite, $CaHPO_4{\cdot}2H_2O$), DCPA (dicalcium phosphate anhydrous, monetite, $CaHPO_4$) or precipitated HA [hydroxyapatite, $Ca_{10}(PO_4)_6(OH)_2$].[17] The addition of calcite powder ($CaCO_3$) to CPC formulations, for instance, of Norian SRS® or Calcibon®, served two purposes: (i) to help form carbonated CaP in the set cement and (ii) to participate in the acid–base neutralization reaction with the acidic calcium phosphate additive (i.e., MCPM, DCPD or DCPA) to *in situ* produce nanocrystals of apatitic CaP or OCP [octacalcium phosphate, $Ca_8(HPO_4)_2(PO_4)_4{\cdot}5H_2O$].[19]

Although the clinically tested CPCs never contained vaterite or aragonite instead of the thermodynamically stable and less soluble calcite in their powder compartments, the experimental synthesis studies of Combes and Rey[20–22] tested the physical, chemical and mechanical properties of mixtures of vaterite with calcium phosphates. The solubility products (i.e., log K_{SP} values) of calcite (−8.48 at 25°C and −8.56 at 37°C), aragonite (−8.33 at 25°C and −8.40 at 37°C) and vaterite (−7.91 at 25°C and −8.05 at 37°C) are well-known.[23]

The interest in the conversion of $CaCO_3$ into apatitic CaP started with the work of Prof. Della M. Roy in the early seventies.[24–26] Roy *et al.*[25,26] investigated the conversion of biogenic coral aragonite (*Porites*) using high temperatures (140°C–260°C) and high autoclave pressures (550–1055 kg/cm^2) in the presence of acidic [such as, $CaHPO_4$ and $Ca(H_2PO_4)_2{\cdot}H_2O$] and basic [such as, $(NH_4)_2HPO_4$] phosphates, as well as of sodium or potassium orthophosphates and acetic acid. Hydrothermal reactions were carried out from 12 to 48 h under the above-mentioned experimental conditions.[27] Characterization studies on biogenic coral, nacre, sea shell and pearl samples having the crystalline phase of aragonite have been extensive and they are left outside the scope of this study, as the organic biomolecules present in such biogenic samples may affect the outcome of *in vitro* testing performed

J. Ferreira—contributing editor

Manuscript No. 34641. Received March 6, 2014; approved June 10, 2014.
*Member, The American Ceramic Society.
†Author to whom correspondence should be addressed. e-mail: c_tas@hotmail.com

in synthetic solutions such as SBFs. CPC development studies need high purity synthetic aragonite and cannot use biogenic aragonites which are forming in the progressively polluted (with heavy metals and cytotoxic industrial chemicals) seas.

Various aragonite synthesis techniques have been reported, just to cite a few, by Bragg,[28] Backstrom,[29] Wray and Daniels,[30] Bills,[31] Ota *et al.*,[32] Wang *et al.*,[33] Ahn *et al.*,[34] Thachepan *et al.*,[35] Park *et al.*,[36] Beck and Andreassen,[37] Sand *et al.*,[38] and Jiang *et al.*[39] The homogeneous precipitation method of Wang *et al.* [33] is used in this study to synthesize aragonite particles.

There are no literature reports for evaluating the stability of synthetic aragonite particles, in the absence of any biopolymers and biomolecules, immersed in any SBF solution at 37°C. As CaP cement paste, containing $CaCO_3$ in it, will rapidly come into contact with the patient's blood, the cement paste developer wishes to employ the least stable form of $CaCO_3$ in the formulation. The ideal cement formulation shall immediately start transforming itself into a CaP phase similar in chemical composition to the bone mineral at the expense of, for example, α-TCP, $CaCO_3$ or brushite present in it. An SBF solution free of nonmetabolic organics such as Tris or Hepes is supposed to simulate the blood plasma and the stability testing of $CaCO_3$ is thus performed in an SBF solution. Similarly, there are no reports on the direct comparison of synthetic calcite, synthetic vaterite and synthetic aragonite particles soaked in an SBF solution under conditions similar to one another.

The soaking of synthetic[40] or biogenic[41,42] aragonite samples in PBS (phosphate buffered saline) solutions of pH 7.4 transformed them into apatitic CaP owing to the high concentration (i.e., 4–40 mM) of phosphorus in such PBS media in comparison to that present in an SBF solution or human blood plasma (i.e., 1 mM). PBS solutions could be useful in converting aragonite completely into apatitic CaP, but not for testing its surface transformation under physiological conditions. Studies assessing biogenic aragonite samples soaked in a Tris-buffered (50 mM) SBF solution are not many,[42–45] yet all reported the deposition of apatite on the biogenic aragonite surface. Tris is the abbreviation for the organic chemical *tris-hydroxymethyl-aminomethane*; $(HOCH_2)_3CNH_2$, which is not present in the human metabolism. The SBF-testing of vaterite (deposited on polyethylene and alumina[46] or in the form of composites embedded in a matrix of poly(lactic) acid[47]) and hydrocortisone-impregnated calcite[48] was again performed in the 50 mM Tris-buffered SBF solutions having a bicarbonate ion concentration of 4.2 mM.

Tris [$(HOCH_2)_3CNH_2$] present in the SBF solution[49,50] received the attention of research as it is able to exert a strong influence on the extent of mineralization. Tris is known to form complexes with various cations, including Ca^{2+} and Mg^{2+}[51] Marques *et al.*[52] and Serro and Saramago[53] reported that in the Tris-buffered SBF solutions, in comparison to those which were Tris-free, a fraction of the Ca^{2+} ions were bound into a stable solution complex and, consequently, less available to deposit CaP on the immersed substrates. Moreover, a study by Rohanova *et al.*[54] stated that the Tris in their SBF solutions was causing an increased dissolution of the surface constituents of bioglass and glass-ceramic samples soaked in it and therefore leading to the premature crystallization of apatite on sample surfaces, tarnishing the reliability of *in vitro* bioactivity tests performed with such Tris-buffered SBF solutions. The amount of Tris used in preparing 1 L of an SBF solution was 6.06 g/L (=50 mM); as this is not a negligible amount, Tris becomes the third most abundant constituent of the SBF solution,[49,50] after 142 mM Na^+ and 148 mM Cl^-.

On the other hand, "lactated Ringer's injection" contains 28 mM Na-*L*-lactate for pH stabilization, but not Tris.[55] Lactated Ringer's injection is preferred in hospitals as an adjunct to the use of whole blood for resuscitation of patients in hemorrhagic shock, in addition to its use in soft tissue injuries, burns and operative trauma.[56] An SBF solution (*Lac*-SBF) perfectly mimicking the inorganic ion concentrations of human blood plasma buffered at pH 7.4 (37°C) containing 22 mM Na-*L*-lactate is used in this study. The same *Lac*-SBF solution was previously used in testing the *in vitro* transformation of brushite at 37°C.[57]

This study was designed to test the hydrothermal stability of synthetic needlelike aragonite particles at human body temperature of 37°C in a Tris-free SBF solution. The *Lac*-SBF solution, in contrast to the 50 mM Tris-buffered SBF solution, perfectly matches all concentrations of the inorganic ions of human blood plasma. Biphasic calcite-vaterite powders were also evaluated in the same *Lac*-SBF solution. Therefore, particles of calcite, vaterite and aragonite have been tested for the first time by the same Tris-free SBF solution.

II. Experimental Procedure

The starting chemicals of calcium chloride dihydrate ($CaCl_2{\cdot}2H_2O$, Thermo Fisher Scientific, Catalog No: C-79, Waltham, MA), magnesium chloride hexahydrate ($MgCl_2{\cdot}6H_2O$, Thermo Fisher, No: AC-19753), sodium bicarbonate ($NaHCO_3$, Thermo Fisher, No: S-233), and urea [$CO(NH_2)_2$, Thermo Fisher, No: U-17] were used in synthesizing the calcium carbonate powders. $CaCl_2{\cdot}2H_2O$, $MgCl_2{\cdot}6H_2O$, $NaHCO_3$, potassium chloride (KCl, Thermo Fisher, No: P-333), sodium chloride (NaCl, Thermo Fisher, No: S-271), sodium sulfate anhydrous (Na_2SO_4, Thermo Fisher, No: S-429), disodium hydrogen phosphate anhydrous (Na_2HPO_4, Thermo Fisher, No: S-374), sodium *L*-lactate [$NaCH_3CH(OH)COO$, Sigma-Aldrich, No: L-7022, St. Louis, MO] and 1 M lactic acid solution ($C_3H_6O_3$, Fluka Analytical, No: 35202, Buchs, Switzerland) were used in preparing the *Lac*-SBF solution.[58] Powder synthesis and SBF-immersion experiments were performed in sterile glass beakers or bottles using preboiled deionized water (18.2 MΩ).

Biphasic calcite-vaterite powders were synthesized by slowly (5 mL/min) adding a 0.275 M sodium bicarbonate solution (6.931 g $NaHCO_3$ dissolved in 150 mL water) to a 0.25 M Ca^{2+} solution (11.026 g $CaCl_2{\cdot}2H_2O$ dissolved in 150 mL water) stirred at 1000 rpm in a 600 mL beaker at room temperature (RT, 22 ± 1°C). Upon completion of the bicarbonate addition, the resultant white suspension was further stirred at 1000 rpm for 1 h at RT. Precipitates were recovered by filtration and washed with 1 L of water, followed by drying at RT for 72 h.

Aragonite particles were synthesized using two different procedures; based on a slight modification of the synthesis process previously described by Wang *et al.*[33] The first aragonite synthesis procedure consisted of dissolving 3.675 g $CaCl_2{\cdot}2H_2O$ (0.25 M Ca^{2+}) and 18.02 g urea (3 M urea) in 100 mL water. The transparent solution was placed into a 100 mL-capacity Pyrex® (Corning Incorporated, Corning, NY) bottle and kept undisturbed (i.e., no stirring or agitation) in an oven at 90°C for 30 h. The first particles were observed to form in the bottles after 3 h of an incubation period. The particles labeled as A-1 were then filtered, washed with 1 L water, and dried at RT for 72 h.

The second aragonite synthesis procedure consisted of dissolving 3.675 g $CaCl_2{\cdot}2H_2O$, 5.083 g $MgCl_2{\cdot}6H_2O$ (0.25 M Mg^{2+}), and 18.02 g urea in 100 mL water. The transparent solution was placed into a 100 mL-capacity Pyrex® bottle and kept undisturbed in an oven at 90°C for 30 h. The first particles started to form after 3 h of an incubation period. The particles labeled as A-2 were then filtered, washed with 1 L water, and dried at RT for 72 h. Mg^{2+} ions are added to the synthesis solutions with the intention of stabilizing the aragonite phase. The procedure presented here for the synthesis of A-2 powders is not previously mentioned in the literature. Both aragonite syntheses produced approximately 10.5 g of particles in 1 L of their mother solutions.

The formation mechanism of aragonite particles, *via* urea decomposition, was described previously by Wang *et al.*,[33] and we refrain from repeating it here in detail. To summarize that mechanism briefly; dissolved urea decomposes, upon heating, first into ammonium cyanate and then into HCO_3^- and CO_3^{2-} ions accompanied by a release of NH_3 (*g*). The urea decomposition causes: (i) a smooth increase in the carbonate concentration of the solution and (ii) the solution pH to rise monotonically to about 8.5–9. Such a monotonic increase in solution pH with urea decomposition[59] would be quite difficult, if not impossible at all, to achieve by external additions of basic solutions of, such as, $(NH_4)_2CO_3$, $NaHCO_3$, Na_2CO_3, NaOH, or KOH.

One liter of the Na-*L*-lactate/lactic acid-buffered SBF solution (i.e., *Lac*-SBF) was prepared by adding the amount of chemicals shown in Table I, in the order given, to 997 mL of preboiled deionized water. Small aliquots of 1 M lactic acid were slowly added using a 1 mL pipette, to gradually decrease the pH to 7.4, at the final step of solution preparation. Freshly prepared *Lac*-SBF solutions had a pH value (7.40 ± 0.01 at both RT and 37°C) similar to that of blood. Inorganic ion concentrations shown in the last column of Table I perfectly matched those of the human blood plasma or extracellular fluid (ECF). Unused portions of *Lac*-SBF were stored in sealed and sterile glass bottles in a refrigerator (+4°C) for a maximum of 3 weeks when not needed.

Biphasic calcite-vaterite powders and aragonite particles (both A-1 and A-2) were soaked at 37°C (±0.05°C) in 100 mL aliquots of *Lac*-SBF solutions, in 100 mL-capacity Pyrex® sealed bottles, for 24, 48, 72 and 96 h periods. Each bottle contained 800 mg of biphasic calcite-vaterite, A-1 or A-2 powders. Bottle contents were not stirred or agitated during the stated soak periods. All supernatant solutions were carefully decanted and then replenished with unused, fresh *Lac*-SBF (preheated to 37°C) at 24 h intervals to partially mimic the blood circulation dynamics of the human body. Soaked powders were finally filtered and washed with 1 L of water, followed by drying at RT for 72 h. The amounts of the *Lac*-SBF-soaked powders obtained were varying between 770 and 790 mg, indicative of quite small losses during solution replenishments.

Visual evaluations of the samples were performed by field emission-scanning electron microscopy (SEM, S-4800, Hitachi, Tokyo, Japan), transmission electron microscopy (TEM, 2010F, Jeol, Tokyo, Japan) and transmitted light optical microscopy (IX-71, Olympus, Tokyo, Japan). The samples for SEM analyses were sputter-coated with a 5 nm-thick layer of Au-Pd alloy prior to imaging at 10 kV. The TEM samples were first suspended in pure ethanol and then dried on copper grids prior to imaging at 200 kV. Chemical analyses of the samples were performed by EDXS (energy-dispersive X-ray spectroscopy, ISIS software, Oxford Instruments, Oxon, UK) and ICP-AES (inductively coupled plasma atomic emission spectroscopy, Model 61E, Thermo Electron, Madison, WI). For the ICP-AES analyses, 20 mg portions of powder samples were dissolved in 3 mL of concentrated HNO_3 solution. Surface areas of powder samples were determined by five-point BET analysis of the nitrogen adsorption isotherm obtained at −196°C after degassing overnight at 30°C (Quantachrome Nova 2000e, Boynton Beach, FL).

Samples for X-ray diffraction (XRD, D-5000, Bruker, Karlsruhe, Germany) runs were first ground in a mortar. All the XRD scans (λ = 1.5406 Å) were performed at 40 KV and 30 mA with a step size of 0.02° and a 5 s count time on a rotating specimen holder. Samples were also analyzed using Fourier-transform infrared spectroscopy (FTIR, Spectrum One, PerkinElmer, MA and Nexus 670, Nicolet, Thermo Scientific) in transmittance and absorbance modes. Powder samples were mixed with KBr (Sigma-Aldrich, Cat. No: 221864) at the ratio of 1 mg sample-to-250 mg KBr in a mortar and pressed into transparent pellets of 7 mm diameter. FTIR data were collected at a resolution of 1 cm^{-1} using 256 scans.

Table I. Preparation of 1 L of Lac-SBF[57,58] Solution

Chemical	Amount (g/L)	Ion	Concentration (mM)
NaCl	5.2599	Na^+	142.0
$NaHCO_3$	2.2682	Mg^{2+}	1.5
KCl	0.3728	K^+	5.0
$MgCl_2{\cdot}6H_2O$	0.3049	Ca^{2+}	2.5
Na_2SO_4	0.0710	HPO_4^{2-}	1.0
$CaCl_2{\cdot}2H_2O$	0.3675	HCO_3^-	27.0
Na_2HPO_4	0.1419	Cl^-	103.0
Na-*L*-lactate	2.4653	SO_4^{2-}	0.5
1 M lactic acid	1.6 mL	*Ca/P molar ratio*	*2.5*

III. Results and Discussion

The SEM photomicrographs of Figs. 1(a) through (c) depict the morphology of the as-prepared biphasic calcite-vaterite, A-1 and A-2 aragonite samples, respectively. A-1 and A-2 samples are optically transparent [Fig. 1(d)]. The biphasic calcite-vaterite powders of this study were synthesized with the intention of using those as a reference for the aragonite particles during the *Lac*-SBF immersion/soaking tests. The characteristic photomicrograph of the sample shown in Fig. 1(a) consisted of agglomerated and partially hollow vaterite spherulites (from 10 to 30 μm in diameter) and 15–20 μm-large calcite rhombohedra. The inset of Fig. 1(a) depicted that (i) the vaterite spherulites were comprised of an intimate aggregation of smaller spheroidal particles (70–150 nm in diameter) and (ii) calcite rhombohedra were crystallizing out of vaterite spherulites. The metastable phase of vaterite can initially form in such aqueous solutions (HCO_3^--to-Ca^{2+} ratio of 1.1) but they are not stable against calcite crystallization at RT during the course of 90 min of synthesis.[60,61] The synthesis of monodisperse spheres[62] and biconvex micropills[63] of vaterite was previously described.

The A-1 [Fig. 1(b)] and A-2 [Figs. 1(c) and (d)] aragonite particles were similar to one another in terms of their dimensions. Although some particles were grown up to 150 μm in length with a width of 5–10 μm, most particles were smaller than those, with the average lengths varying between 30 and 70 μm. In brief, the mean aspect ratio of the particles of A-1 and A-2 aragonite samples was around 10. If we were performing the synthesis reaction at 70°C, instead of 90°C of this study, the aragonite particles were found to be more uniform in size and aspect ratio,[64] however, the low temperature samples contained small amounts of the secondary phase of calcite. To increase the process yield, the aragonite synthesis procedure of this study significantly increased the urea concentration (from 0.75 to 3 M) and the reaction time (from 1 to 30 h) at 90°C in comparison to the original urea decomposition method reported by Wang *et al.*[33]

FTIR and XRD data of the as-prepared biphasic calcite-vaterite and aragonite samples (both A-1 and A-2) are shown in Figs. 2(a) through (d). The IR bands of the biphasic calcite (e.g., 713 cm^{-1})-vaterite (e.g., 745 cm^{-1}) sample [Fig. 2(a)] conformed well to the FTIR evaluation of Andersen and Kralj[65] on biphasic calcite-vaterite mixtures.

Analyses of the XRD data of the biphasic calcite-vaterite mixtures [Fig. 2(b)] indicated the presence of rhombohedral calcite (space group *R*-3*c*, 167) with the hexagonal lattice parameters of $a = 4.99$ and $c = 17.06$ Å (ICDD PDF 5-0586) and hexagonal vaterite (space group $P6_3/mmc$, 194) having the lattice parameters of $a = 7.147$ and $c = 16.93$ Å (ICDD PDF 33-0268 or 60-0483). The direct determination of the volume percentage of calcite in such mixtures using the XRD peak intensities could be misleading as there happens to be a

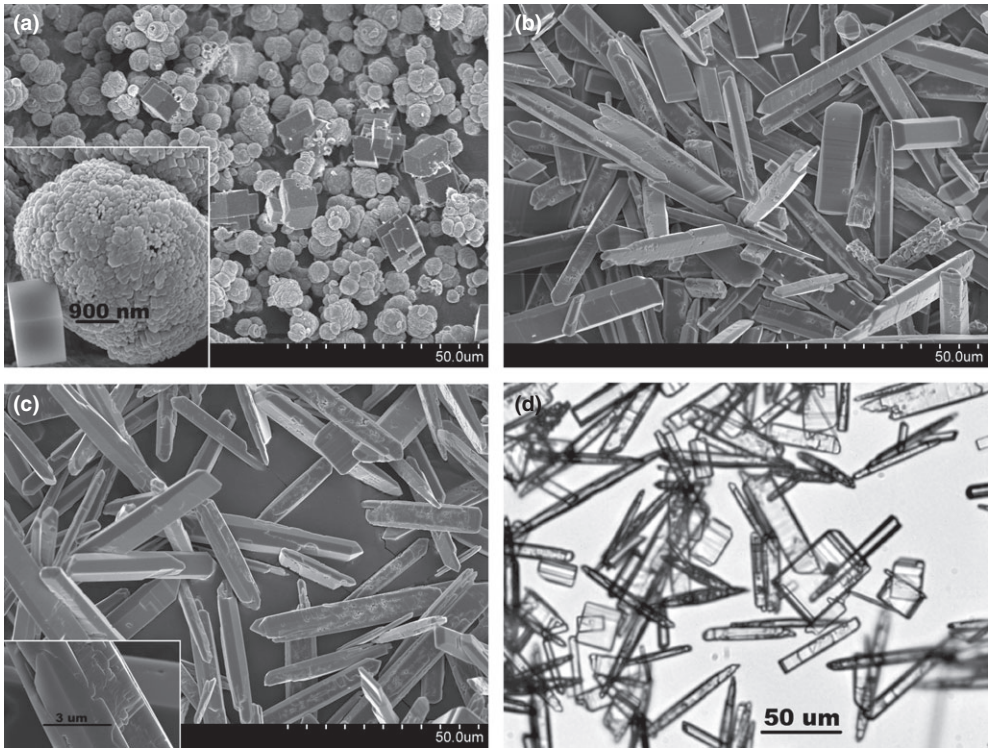

Fig. 1. Photographs of (a) calcite-vaterite, (b) A-1, and (c–d) A-2 samples.

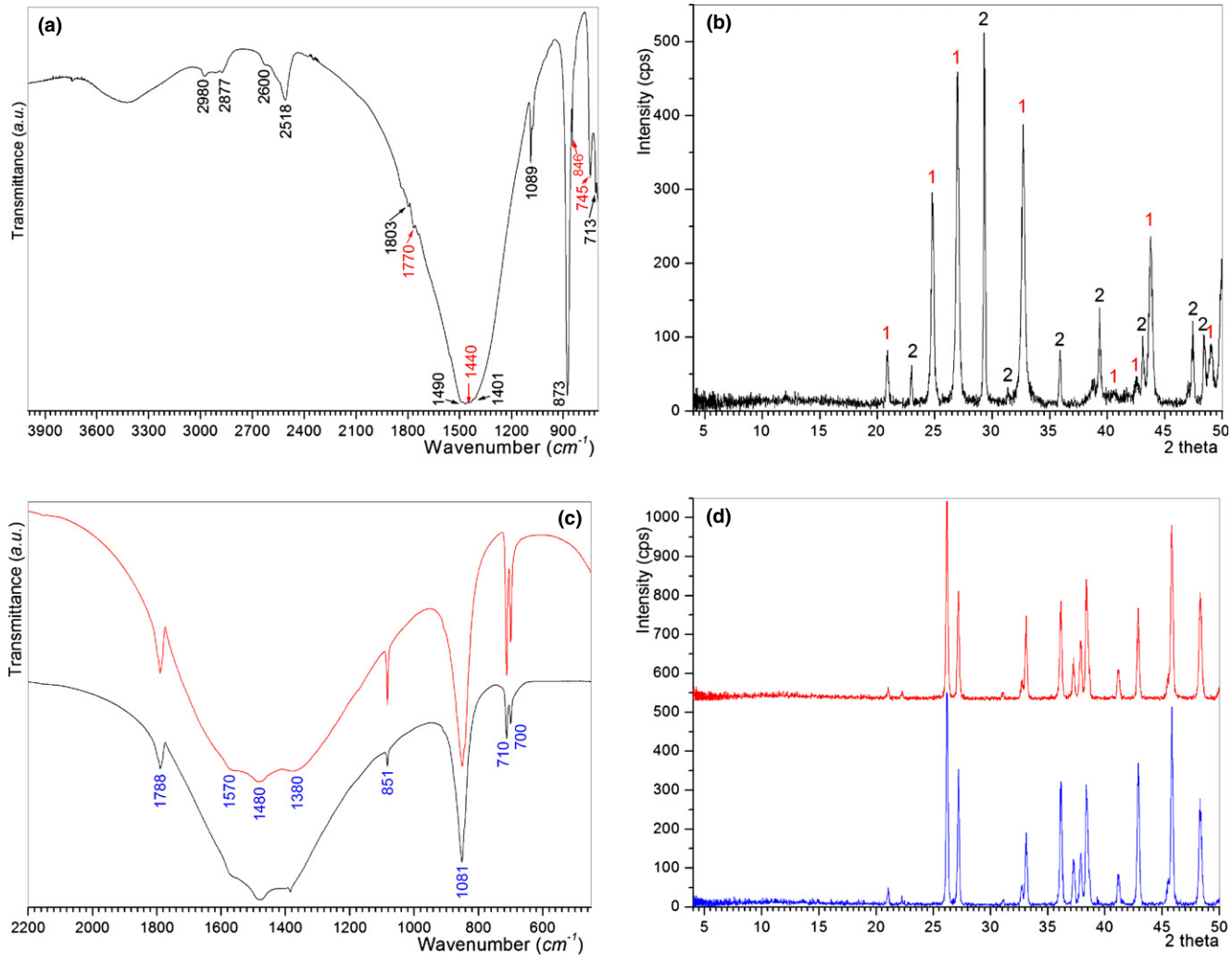

Fig. 2. (a) FTIR of biphasic calcite-vaterite, calcite (numbers in black), vaterite (red); (b) XRD of calcite-vaterite, 1: vaterite, 2: calcite peaks; (c) FTIR of A-1 (blue) and A-2 (red); (d) XRD of A-1 (blue) and A-2 (red) samples.

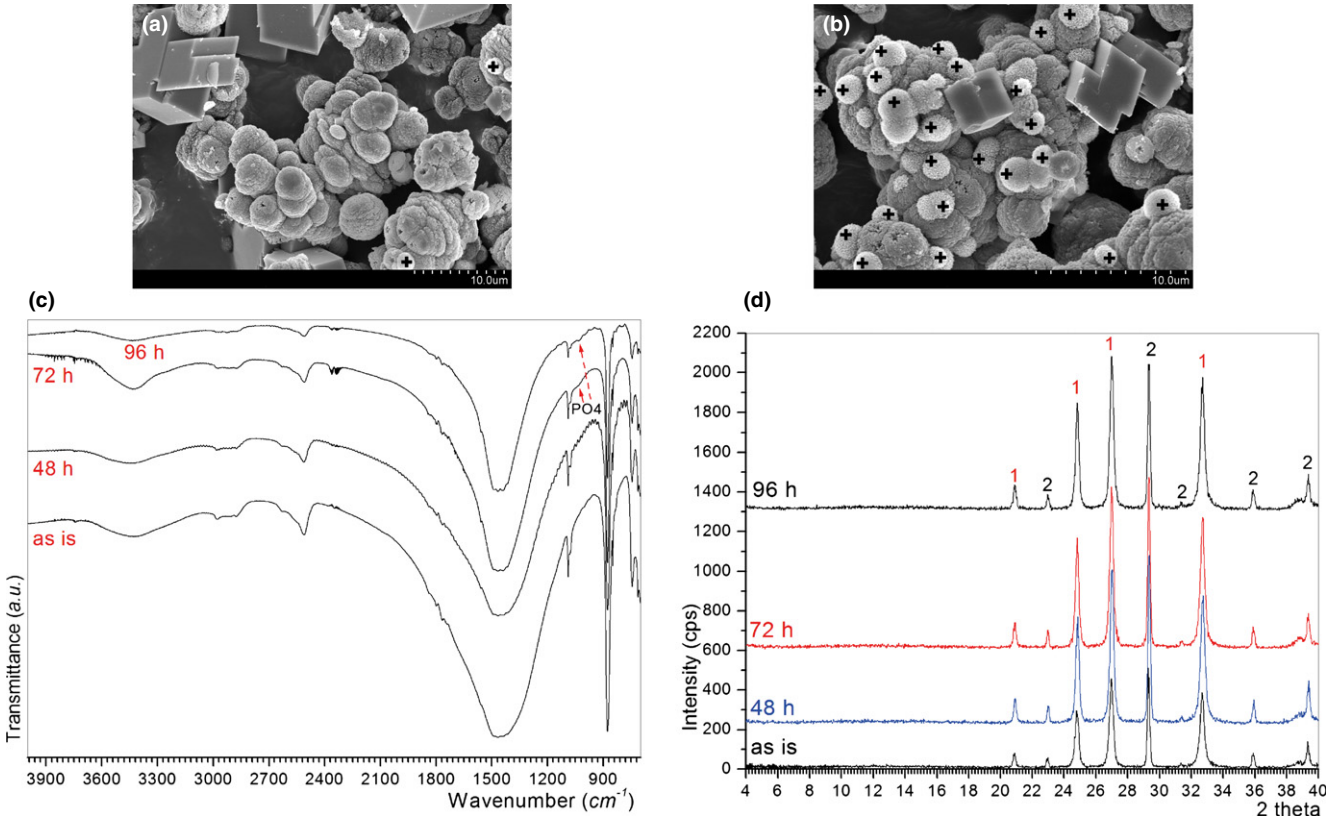

Fig. 3. (a) SEM images of biphasic calcite-vaterite in *Lac*-SBF for 72 h; (b) biphasic calcite-vaterite in *Lac*-SBF for 96 h, + signs denote the apatitic CaP globules; (c) FTIR and (d) XRD data of biphasic calcite-vaterite in *Lac*-SBF, 1: vaterite, 2: calcite peaks.

significant difference between the crystallinity of precipitated calcite rhombohedra and vaterite spherulites. Such determinations could be performed by preparing known quantities of physically mixed pure calcite and pure vaterite powders, followed by a number of XRD runs. The presence of distinct calcite rhombohedra and vaterite spherulites in the sample of Fig. 1(a) and Figs. 2(a) and (b) was sufficient for our purposes, as the next step of this study would only examine the apatitic CaP-inducing ability of such rhombohedra and spherulites at 37°C in a Tris-free SBF solution.

FTIR [Fig. 2(c)] and XRD [Fig. 2(d)] data of A-1 and A-2 samples were quite similar to one another and they indicated the presence of single-phase orthorhombic aragonite (space group *Pmcn*, 62) with the lattice parameters of $a = 4.962$, $b = 7.968$, $c = 5.744$ Å (ICDD PDF 41-1475). Infrared bands of aragonite shown in Fig. 2(c) match those reported by Andersen and Brecevic.[66] Both samples had a BET surface area of 0.3 m^2/g. The EDXS analyses performed on the A-2 sample, which is produced in an equimolar (0.25 M each) Ca^{2+}-Mg^{2+} solution, failed to detect any magnesium in the A-2 aragonite particles. ICP-AES analyses, on the other hand, revealed the presence of 1050 ± 30 ppm magnesium in the A-2 samples. The sample characterization procedures of this study were not able to determine the fractions of surface adsorbed and lattice incorporated magnesium found in the A-2 samples. Koga and Nishikawa[67] reported the presence of 4200 ppm magnesium in coral aragonite. While the coral skeletons are formed in seawater rich in Mg^{2+} (i.e., 55 mM[68]), over an extended period of time, the A-2 synthesis procedure of this study was able to incorporate magnesium into the aragonite particles in a relatively short period of time of 30 h at 90°C.

The *Lac*-SBF solution, without using an excessive amount of Tris (50 mM) as the conventional SBF solutions do, perfectly matches the inorganic ion concentrations of blood plasma, and *Lac*-SBF is used to evaluate the response of $CaCO_3$ powders to an inorganic solution mimicking blood plasma under the biomimetic conditions of 37°C and pH 7.4. It was difficult to spot any apatitic CaP globules on biphasic calcite-vaterite samples soaked in the *Lac*-SBF solution for 24 and 48 h. However, those apatitic CaP globules started to slowly form only on vaterite spherulites of the 72 h sample and grew more in the 96 h sample, as shown in the SEM images of Figs. 3(a) and (b). Surfaces of calcite rhombohedra remained clear of any such globules. Ikoma *et al.* [48] reported the complete covering of calcite surfaces by apatitic CaP globules only when they used a special Tris-buffered solution (of pH 8, but not 7.4) containing only 2.5 mM Ca^{2+}, 1 mM HPO_4^{2-}, 284 mM Na^+ and 296 mM Cl^-. Kim and Park,[69] on the other hand, reported that pure calcite rhombohedra soaked in a 1.5× Tris-SBF solution for 48 h (at 37°C) only exhibited a very small amount of apatitic CaP globules forming on their surfaces.

The characteristic phosphate band observed at around 1030 cm^{-1} in the FTIR spectra of Fig. 3(c) proved the CaP formation. XRD traces of the *Lac*-SBF-soaked biphasic calcite-vaterite samples were not able to show any apatitic CaP peaks. XRD could not show any peaks (for instance the one at 25.89° 2θ for the (002) reflection of apatite) for such apatitic CaP globules of quite low crystallinity. Only the XRD traces of samples remaining in any SBF solution for several weeks would then exhibit low intensity peaks for the (002) reflection of apatite;[50] it is a matter of maturation of either amorphous or cryptocrystalline CaP initially forming at the human body temperature (37°C) in such physiological solutions. The morphology of the apatitic CaP globules of Fig. 3(b) resembled those formed in the SBF solution on metals, ceramics and polymers.[49]

If the apatitic CaP globules were first forming in the *Lac*-SBF solution and then simply precipitating on the available surfaces as a result of gravitational sedimentation, then the surfaces of the calcite rhombohedra should have been cov-

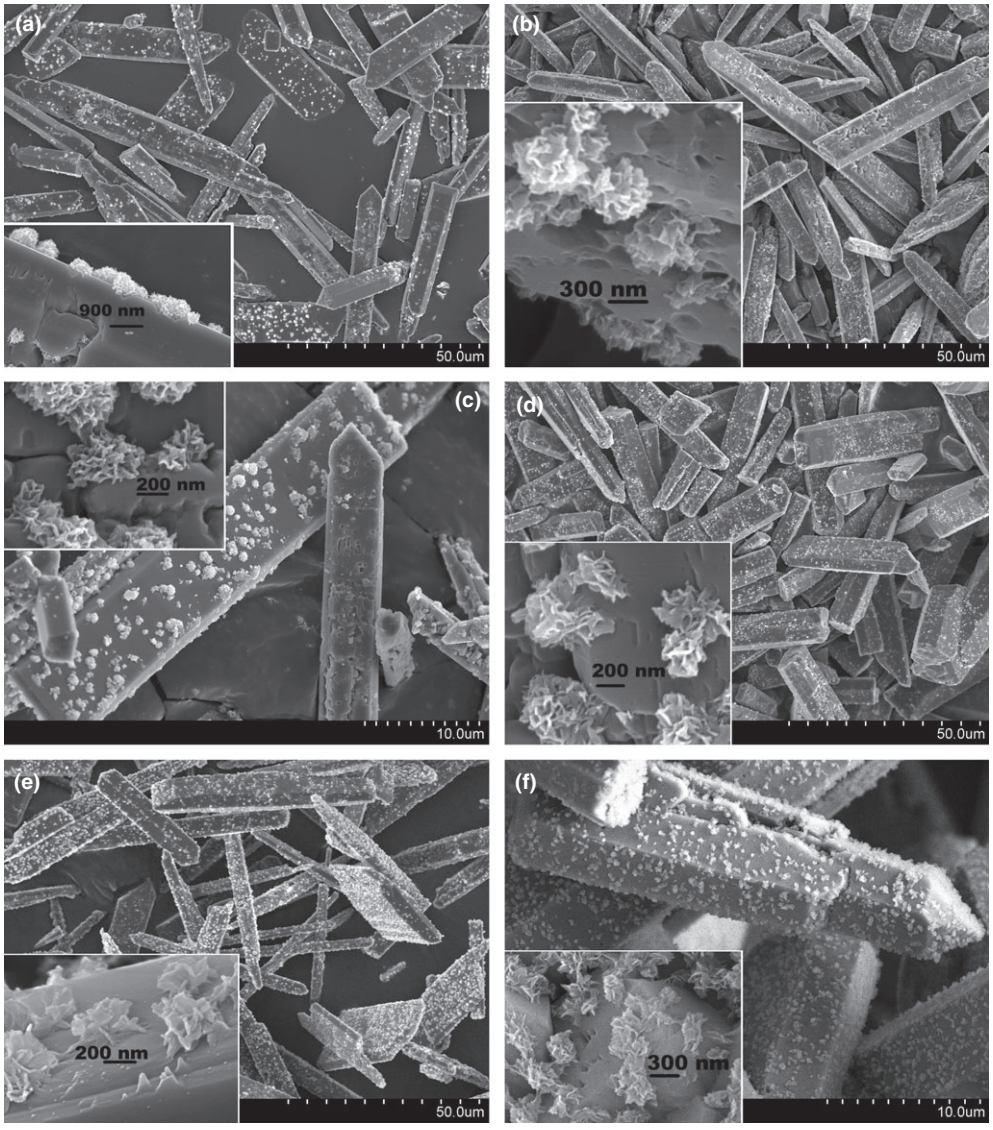

Fig. 4. (a), (c) and (e): SEM images of A-1 aragonite particles soaked in *Lac*-SBF for 48, 72 and 96 h, respectively; (b), (d) and (f): SEM images of A-2 aragonite particles soaked in *Lac*-SBF for 48, 72 and 96 h, respectively.

ered with those as well. Therefore, this hypothesis is simply negated by the SEM images of Figs. 3(a) and (b). The calcite rhombohedra did not have the apatitic CaP-inducing ability, up to the end of the first 96 h in *Lac*-SBF at 37°C, in direct comparison to the co-existing vaterite spherulites. The *Lac*-SBF solution had the unique property of being free of any Tris-buffer. Therefore, it was free of any complications reported by Rohanova *et al.*[54] It may be speculated that the surfaces of calcite rhombohedra remain thermodynamically stable and do not release any Ca^{2+} to tip over the delicate molar balance of Ca^{2+}/HPO_4^{2-} of 2.5 of the *Lac*-SBF solution. The difference in the log K_{SP} values of calcite (−8.56) and vaterite (−8.05) has been mentioned above. The first important finding of this study is that the calcite rhombohedra in the biphasic calcite-vaterite samples do not have the apatitic CaP-inducing ability during their first 96 h of stay in the *Lac*-SBF solution.

SEM photomicrographs of Fig. 4 present a direct comparison of A-1 (pure) and A-2 (with 1050 ppm Mg) aragonite particles as a function of soaking time in *Lac*-SBF at 37°C. A-1 and A-2 samples soaked for 24 h did not display any noticeable change in particle morphology from those shown in Figs. 1(b) and (c).

Carnation-like deposits of CaP formed on the surfaces of both A-1 and A-2 aragonite samples started to form somewhere between 24 and 48 h of soaking in the *Lac*-SBF solution. The vaterite spherulites of the biphasic calcite-vaterite samples, on the other hand, started to form globular deposits on their surfaces sometime between 48 and 72 h of stay in the same solution. The second important finding of this study was that the vaterite spherulites present in a biphasic calcite-vaterite sample were more sluggish, in comparison to aragonite particles, to react with the physiological solution at 37°C during the first 48 h of immersion.

The globular deposits of CaP seen on vaterite spherulites, after 96 h at 37°C, in *Lac*-SBF [in Fig. 3(b)] are quite different in morphology from the carnation-like CaP deposits observed on the aragonite samples of 96 h [Figs. 4(e) and (f)]. The same physiological solution used for evaluating the biphasic calcite-vaterite and synthetic aragonite samples seemed to be sensitive to the surface it is acting on and seemed to change the morphology of the CaP formed. The carnation-like deposits observed on the aragonite samples was shown to originate from the solid surface and growing toward the solution side (insets of Fig. 4).

FTIR and XRD data of the A-1 and A-2 aragonite particles soaked in the *Lac*-SBF solution at 37°C are presented in Fig. 5. The FTIR data of Figs. 5(a) and (b) were collected in the absorbance mode with a different spectrophotometer so that they look a bit different from the IR traces shown in

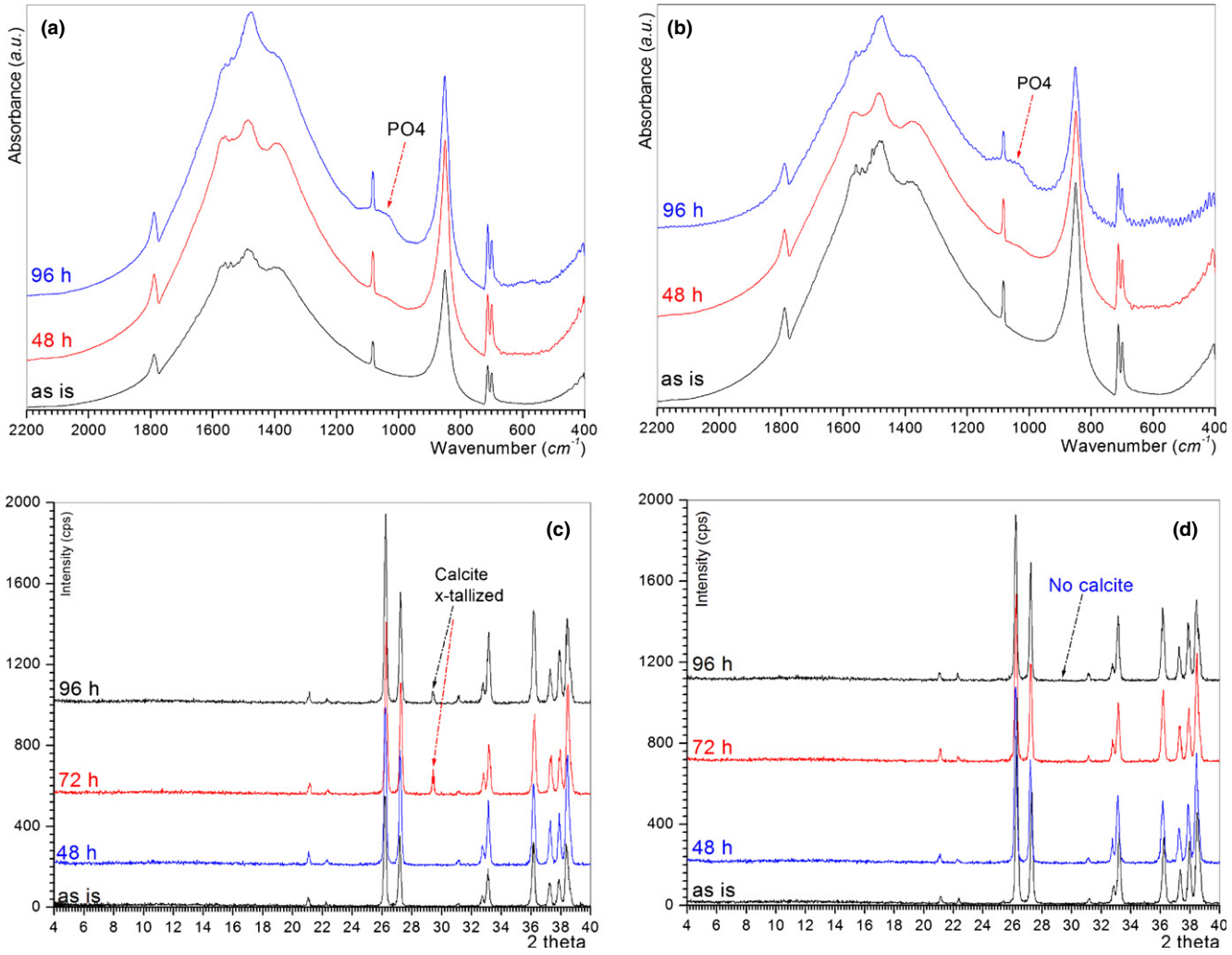

Fig. 5. (a) and (b): FTIR data of A-1 and A-2 aragonite soaked in Lac-SBF at 37°C, respectively; (c) and (d): XRD traces of A-1 and A-2 aragonite soaked in *Lac*-SBF at 37°C, respectively.

Figs. 2 and 3 (transmittance mode). However, the data collection mode did not affect the information gathered. Both A-1 and A-2 aragonite samples displayed the characteristic 1030 cm^{-1} phosphate bands in their FTIR data [Figs. 5(a) and (b)], starting from the 48 h samples. XRD traces of both A-1 and A-2 [Figs. 5(c) and (d)] did not display the (002) reflection of apatite at 25.89°2θ, meaning that those carnation-like apatitic CaP deposits of Fig. 4 were of quite low crystallinity. Mg-doped (1050 ppm) aragonite samples (i.e., A-2) were stable against transformation into calcite in the *Lac*-SBF solution [Fig. 5(d)]. Pure aragonite samples (A-1) partially transformed into calcite [Fig. 5(c)] at some time between 48 and 72 h of immersion in the *Lac*-SBF solution. This has been the third significant finding of this study. The observation was that synthetic aragonite can be stabilized by small amounts of Mg doping as, for instance, biogenic coral skeletons and sea shells are able to accomplish.[67]

A robust method to assess the extent of carnation-like apatitic CaP formation on the aragonite particles, as a function of immersion time in the *Lac*-SBF solution at 37°C, is the measurement of the BET (Brunauer-Emmett-Teller) surface area. The as-prepared A-2 aragonite particles [Figs. 1(c) and (d)], which are stable against undesired calcite formation in the *Lac*-SBF solution, were found to have a BET surface area of 0.3 m^2/g. This value did not change at all after 24 h of immersion in the *Lac*-SBF solution; however, it first increased to 0.79 m^2/g after 48 h and then to 1.98 m^2/g at the end of 96 h [Fig. 4(f)]. In other words, the BET surface area of the A-2 aragonite (with 1050 ppm Mg) particles increased by 560% after 4 d in the *Lac*-SBF solution.

TEM photomicrographs of Fig. 6 shed light on the crystallinity of the carnation-like apatitic CaP deposits formed on A-2 aragonite (with 1050 ppm Mg) samples soaked in the *Lac*-SBF solution for 96 h at 37°C. Figure 6(a) shows one of such deposits at low magnification and indicate two points of interest for further study. The first area, labeled 1 in Fig. 6(a), turned out to be completely amorphous [Fig. 6(b)]. The second area, labeled 2 in Fig. 6(a), was of very low crystallinity [Fig. 6(c)]; such materials may be called to be cryptocrystalline. The passage from a completely amorphous to a cryptocrystalline material, in moving from the solution-side to the particle-side of the shown deposit represents a process of maturation taking place in the physiological solution of this study. The solution-side (or edge) of that deposit [Figs. 6(a) and (b)] denotes the newly-formed apatitic CaP. The parts of the same deposit which is located nearby that large aragonite particle (seen black in Fig. 6(a) due to its thickness) represent the first-formed apatitic CaP. Physiological solutions, such as *Lac*-SBF, which contain 25-27 mM HCO_3^-, 142 mM Na^+, 2.5 mM Ca^{2+}, 1.5–3 mM Mg^{2+}, 1 mM HPO_4^{2-}, and 103–125 mM Cl^- have been reported to form amorphous CaP at 37°C and pH 7.4, but not crystalline hydroxyapatite.[70,71]

Uan *et al.*[72] observed the formation of aragonite (together with minor amounts of calcite) when testing the corrosion resistance of AZ91D (Mg-9 wt% Al-1 wt% Zn)-type Mg alloys in a *Tris*-SBF solution, noting the role of Mg in favoring the aragonite formation over calcite. Cheng *et al.*[73] noted that at low concentrations (<24 mM), Mg^{2+} is able to modify the habit to form calcite with a rhombohedral shape;

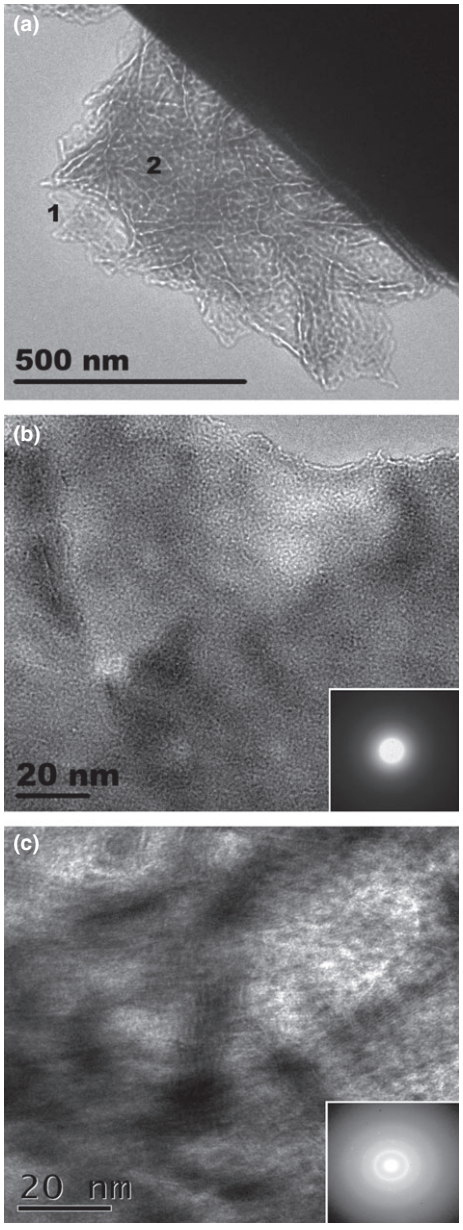

Fig. 6. (a) Low magnification TEM photomicrograph of a carnation-like apatitic CaP deposit formed on the surface of an A-2 aragonite (w/1050 ppm Mg) particle soaked in *Lac*-SBF for 96 h at 37°C; (b) point 1 of (a) with its selected area electron diffraction (SAED) image in the inset; (c) point 2 of (a) with its SAED.

while at higher concentrations, approaching that of seawater (55.5 mM), the calcite would be mostly inhibited, thus enabling the formation of aragonite for coral skeletons and sea shells. As Mg^{2+} ions are strongly hydrated, they disturb the growth of calcite nuclei such that Mg-stabilized aragonite is preferentially precipitated rather than calcite if $[Mg^{2+}]$: $[Ca^{2+}]$ >4:1.[74,75] Ca^{2+} concentration of modern seawater is 10.8 mM;[68] therefore, this ratio is always greater than 5 in aqueous media in which coral skeletons (having 4200 ppm Mg[67]) and sea shells are formed.

The preferred morphology of a crystal (such as calcite, vaterite or aragonite) is usually determined by the surface energy and the related growth rate of various crystallographic planes. Calcite rhombohedra (with a theoretical density of 2.711 g/cm^3) almost always expose their hydrated (10.4) planes of lowest free energy, which are oxygen terminated surface planes.[76,77] Vaterite (2.665 g/cm^3) and aragonite (2.927 g/cm^3) crystals, on the other hand, typically present their low surface free energy (010) planes and both of these (010) vaterite and aragonite planes are Ca terminated planes. Interestingly, all other possible surface planes of vaterite and aragonite are also Ca-terminated planes.[76] The oxygen terminated (10.4) surface planes of calcite rhombohedra most probably explain their inability to induce apatitic CaP formation [Figs. 3(a) and (b)], as the CaP formation in SBF solutions require the localized disturbance of the Ca/P molar ratio (2.5, also that of the human blood) of the solution by the release of Ca^{2+} ions from the solid surface. In human metabolism, on the other hand, the presence of blood glycoproteins (e.g., Fetuin-A) prevents the pathological calcium phosphate nucleation all over the body by forming nanosize calciprotein particles.[78]

The use of calcite as an additive in calcium phosphate cements (CPCs), such as Calcibon®, Biopex®, Rebone® and Norian SRS®, is designed for the rapid acid–base neutralization reaction to take place between particles of calcite and one of the mildly acidic calcium phosphate (e.g., brushite or monetite) also present in the above-mentioned cement formulations. When this happens to be the case, the careful selection of $CaCO_3$ from calcite, vaterite, or aragonite unfortunately became irrelevant as the acidic CaP component of the CPC would instantly react with any such form of $CaCO_3$ present in the cement powder and dissolve it to locally form seed crystals of apatitic and carbonated CaP. This study has shown that needles of aragonite and spherulites of vaterite are able to form, by themselves, apatitic CaP on their surfaces at pH, ionic environment and temperature conditions similar to those of the human body. Such Mg-doped aragonite particles can be combined with Zn- and/or F-doped amorphous CaP powders[79,80] to develop a new family of resorbable cement pastes or inorganic bio-inks suitable for 3D printing applications.

Oral and orthopedic surgeons need resorbable CPCs. The resorbability of implantable bioceramics, such as $CaCO_3$, HA or β-TCP [β-tricalcium phosphate, β-$Ca_3(PO_4)_2$], can only be tested by osteoclast cells, and by further *in vivo* and clinical studies. In a healthy human, the old bones are first eroded by the osteoclast cells and the erosion pits created by osteoclasts are then filled with new bone deposited by the osteoblast cells; this well-orchestrated process happens on a daily basis. Monchau *et al.*[81] studied the *in vitro* resorption of the surfaces of all three of the above bioceramics using human osteoclast cells, quantified the zones of degradation/erosion (in μm^2) after 48 h of osteoclast culture, and reported that $CaCO_3$ has the highest (7521 μm^2) and β-TCP has the lowest (2939 μm^2) degraded surface. This is the only study in literature that simultaneously compared these bioceramics using osteoclasts. However, the high resorbability of $CaCO_3$ was not surprising and was expected. Implanted bioceramics must be replaced with new biological bone formation in less than a year and such bioceramics should not remain in tissues as nonabsorbable materials.

Osteoclast cell culture studies on Mg-doped and pure synthetic aragonite are needed to further assess the viability of using synthetic aragonite powders in new CPC formulations. Geblinger *et al.*[82] studied the resorption of calcite using the osteoclast cells and reported that the surface roughness and nano-topography of the calcite surface affects the size and shape of the erosion pits. In a study of the osteoclastic resorption of nacre-type aragonite (from oyster mother of pearl) in direct comparison to bovine cortical bone, Duplat *et al.*[83] observed osteoclastic resorption of nacre. Fricain *et al.*[84] tested porous coral aragonite and porous calcite (obtained by heating the former at 500°C for 15 h in air) using bone marrow cells and found that both aragonite and calcite samples produced similar cell proliferation patterns and similar alkaline phosphatase (ALP) activity values. Even though a significant number of *in vivo* studies[85–88] were also performed with coral- and nacre-type biogenic aragonite, we were not able to spot any *in vitro* or *in vivo* studies performed on synthetic aragonite; possibly indicating a

surprising lack of interest in synthetic aragonite in hard tissue repair and bone tissue engineering applications.

IV. Conclusions

Tris [$(HOCH_2)_3CNH_2$], which is not found in human blood or metabolism, has been commonly used (at a high concentration of 50 mM) to buffer conventional SBF (simulated/synthetic body fluid) solutions at pH 7.4 and 37°C. This study reached the below conclusions using a Tris-free, Na-*L*-lactate (22 mM)-buffered *Lac*-SBF solution to test the hydrothermal stability of all three crystalline polymorphs of calcium carbonate, namely, synthetic calcite, vaterite, and aragonite.

1. The surfaces of calcite rhombohedra, present in a biphasic calcite-vaterite sample, remained completely inert to the *Lac*-SBF solution even after 96 h of immersion at 37°C.
2. Vaterite spherulites, present in a biphasic calcite-vaterite sample, accrued on their surfaces a significant amount of apatitic CaP globules between 72 and 96 h of immersion in the *Lac*-SBF solution at 37°C.
3. Needle-like synthetic aragonite particles doped with 1050 ppm Mg remained stable against calcite crystallization during the 96 h of immersion in the *Lac*-SBF solution, whereas pure aragonite particles partially transformed into calcite starting after the 48th h.
4. The BET surface areas of Mg-doped aragonite particles increased by about 560% (from 0.3 to 1.98 m^2/g) upon 96 h of immersion in the *Lac*-SBF solution at 37°C.
5. Both pure and Mg-doped synthetic aragonite particles formed carnation-like amorphous CaP deposits on their surfaces starting between 24 and 48 h of immersion in the *Lac*-SBF solution at 37°C, whose morphology was different from those deposited on the surfaces of vaterite spherulites.
6. Synthetic aragonite, in comparison to calcite, is not inert to a physiological solution, such as *Lac*-SBF, perfectly mimicking the pH, temperature and inorganic ionic environment of the human blood plasma.

Notes

Certain commercial instruments or materials are identified in this article solely to foster understanding. Such identification does not imply recommendation or endorsement by the authors, nor does it imply that the instruments or materials identified are necessarily the best available for the purpose.

Acknowledgments

The authors are grateful for the generous help of Mr. Jongmin Youn and Dr. Moonsub Shim of UIUC in letting us to use their FTIR spectrophotometer to collect the FTIR data of Figs. 5(a) and (b). This work was partially supported by an AFOSR grant no. 919 AF Sub TX UTA II-000843. This research was carried out in part in the Frederick Seitz Materials Research Laboratory Central Facilities, University of Illinois at Urbana-Champaign, which were partially supported by the US Department of Energy under grants DE-FG02-07 ER 46453 and DE-FG02-07 ER 46471.

References

[1]S. Mann, *Biomineralization: Principles and Concepts in Bioinorganic Materials Chemistry*. Oxford University Press, Oxford, 2001.

[2]V. C. Allison, "The Growth of Stalagmites and Stalactites," *J. Geol*, **31**, 106–25 (1923).

[3]C. M. Sherwin and J. U. L. Baldini, "Cave Air and Hydrological Controls on Prior Calcite Precipitation and Stalagmite Growth Rates: Implications for Palaeoclimate Reconstructions Using Speleothems," *Geochim. Cosmochim. Acta*., **75**, 3915–29 (2011).

[4]Y. Kojima, A. Kawanobe, T. Yasue, and Y. Arai, "Synthesis of Amorphous Calcium Carbonate and Its Crystallization," *J. Ceram. Soc. Jpn*., **101**, 1145–52 (1993).

[5]L. Brecevic and D. Kralj, "On Calcium Carbonates: From Fundamental Research to Application," *Croat. Chem. Acta*., **80**, 467–84 (2007).

[6]H. Vater, "Ueber den Einfluss der Loesungsgenossen auf die Krystallisation des Calciumcarbonates," *Z. Kristallogr. Mineral*, **27**, 477–512 (1897).

[7]A. C. Tas, "A New Calcium Phosphate Cement Composition and a Method for the Preparation Thereof," US Patent 6,929,692 (August 16, 2005); Canadian Patent 2,438,742 (August 9, 2011); European Patent 1,394,132 (September 12, 2012).

[8]W. Castro, "Elemental Analysis of Biological Matrices by Laser Ablation High Resolution Inductively Coupled Plasma Mass Spectrometry (LA-HR-ICP-MS) and High Resolution Inductively Coupled Plasma Mass Spectrometry (HR-ICP-MS)"; Ph.D. Thesis, Florida International University, Miami, Florida, 2008.

[9]T. D. Driskell, A. L. Heller, and J. F. Koenigs, "Dental Treatments"; US Patent 3,913,229, October 21, 1975.

[10]M. P. Ginebra, E. Fernandez, F. C. M. Driessens, and J. A. Planell, "Modeling of the Hydrolysis of α-Tricalcium Phosphate," *J. Am. Ceram. Soc*., **82**, 2808–12 (1999).

[11]R. I. Martin and P. W. Brown, "Hydration of Tetracalcium Phosphate," *Adv. Cement Res*., **5**, 119–25 (1993).

[12]H. Monma, M. Goto, H. Nakajima, and H. Hashimoto, "Preparation of Tetracalcium Phosphate," *Gypsum Lime*, **202**, 151–5 (1986).

[13]M. Tamai, T. Isshiki, K. Nishio, M. Nakamura, A. Nakahira, and H. Endoh, "Transmission Electron Microscopic Studies on an Initial Stage in the Conversion Process From α-Tricalcium Phosphate to Hydroxyapatite," *J. Mater. Res*., **18**, 2633–8 (2003).

[14]W. C. Chen, J. H. C. Lin, and C. P. Ju, "Transmission Electron Microscopic Study on Setting Mechanism of Tetracalcium Phosphate/Dicalcium Phosphate Anhydrous-Based Calcium Phosphate Cement," *J. Biomed. Mater. Res*., **64**, 664–71 (2003).

[15]A. Almirall, G. Larrecq, J. A. Delgado, S. Martinez, J. A. Planell, and M. P. Ginebra, "Fabrication of Low Temperature Macroporous Hydroxyapatite Scaffolds by Foaming and Hydrolysis of an α-TCP Paste," *Biomaterials*, **25**, 3671–80 (2004).

[16]L. E. Carey, H. H. K. Xu, C. G. Simon, S. Takagi, and L. C. Chow, "Premixed Rapid-Setting Calcium Phosphate Composites for Bone Repair," *Biomaterials*, **26**, 5002–14 (2005).

[17]M. Bohner, U. Gbureck, and J. E. Barralet, "Technological Issues for the Development of More Efficient Calcium Phosphate Bone Cements: A Critical Assessment," *Biomaterials*, **26**, 6423–9 (2005).

[18]S. Jalota, S. B. Bhaduri, and A. C. Tas, "Synthesis of HA-Seeded TTCP ($Ca_4(PO_4)_2O$) Powders at 1230°C From $Ca(CH_3COO)_2{\cdot}H_2O$ and $NH_4H_2PO_4$," *J. Am. Ceram. Soc*., **88**, 3353–60 (2005).

[19]M. P. Ginebra, M. Espanol, E. B. Montufar, R. A. Perez, and G. Mestres, "New Processing Approaches in Calcium Phosphate Cements and Their Applications in Regenerative Medicine," *Acta Biomater*., **6**, 2863–73 (2010).

[20]C. Combes, B. Miao, R. Bareille, and C. Rey, "Preparation, Physical-Chemical Characterisationa and Cytocompatibility of Calcium Carbonate Cements," *Biomaterials*, **27**, 1945–54 (2006).

[21]C. Combes, R. Bareille, and C. Rey, "Calcium Carbonate-Calcium Phosphate Mixed Cement Compositions for Bone Reconstruction," *J. Biomed. Mater. Res*., **79A**, 318–28 (2006).

[22]S. Tadier, R. Bareille, R. Siadous, O. Marsan, C. Charvillat, S. Cazalbou, J. Amedee, C. Rey, and C. Combes, "Strontium-Loaded Mineral Bone Cements as Sustained Release Systems: Compositions, Release Properties, and Effects on Human Osteoprogenitor Cells," *J. Biomed. Mater. Res*., **100B**, 378–90 (2012).

[23]L. N. Plummer and E. Busenberg, "The Solubilities of Calcite, Aragonite and Vaterite in CO_2-H_2O Solutions Between 0 and 90°C, and an Evaluation of the Aqueous Model for the System $CaCO_3$-CO_2-H_2O," *Geochim. Cosmochim. Acta*, **46**, 1011–40 (1982).

[24]D. M. Roy and S. K. Linnehan, "Hydroxyapatite Formed From Coral Skeletal Carbonate by Hydrothermal Exchange," *Nature*, **246**, 220–2 (1974).

[25]D. M. Roy, W. Eysel, and D. Dinger, "Hydrothermal Synthesis of Various Carbonate-Containing Calcium Hydroxyapatite," *Mater. Res. Bull*., **9**, 35–40 (1974).

[26]D. M. Roy, "Porous Biomaterials and Method of Making Same"; US Patent 3,929,971, December 30, 1975.

[27]A. C. Tas, "Porous, Biphasic $CaCO_3$-Calcium Phosphate Biomedical Cement Scaffolds From Calcite ($CaCO_3$) Powder," *Int. J. Appl. Ceram. Technol*., **4**, 152–63 (2007).

[28]W. L. Bragg, "The Structure of Aragonite," *Proc. R. Soc. A (London)*, **105**, 16–39 (1924).

[29]H. L. J. Backstrom, "The Thermodynamic Properties of Calcite and Aragonite," *J. Am. Chem. Soc*., **47**, 2432–42 (1925).

[30]J. L. Wray and F. Daniels, "Precipitation of Calcite and Aragonite," *J. Am. Chem. Soc*., **79**, 2031–4 (1957).

[31]P. M. Bills, "The Precipitation of Calcium Carbonate Polymorphs *In Vitro* at 37°C," *Calcif. Tissue Int*., **37**, 174–7 (1985).

[32]Y. Ota, S. Inui, T. Iwashita, T. Kasuga, and Y. Abe, "Preparation of Aragonite Whiskers," *J. Am. Ceram. Soc*., **78**, 1983–4 (1995).

[33]L. Wang, I. Sondi, and E. Matijevic, "Preparation of Uniform Needle-Like Aragonite Particles by Homogeneous Precipitation," *J. Coll. Interf. Sci*., **218**, 545–53 (1999).

[34]J. W. Ahn, K. S. Choi, S. H. Yoon, and H. Kim, "Synthesis of Aragonite by the Carbonation Process," *J. Am. Ceram. Soc*., **87**, 286–8 (2004).

[35]S. Thachepan, M. Li, S. A. Davis, and S. Mann, "Additive-Mediated Crystallization of Complex Calcium Carbonate Superstructures in Reverse Microemulsions," *Chem. Mater*., **18**, 3557–61 (2006).

[36]W. K. Park, S. J. Ko, S. W. Lee, K. H. Cho, J. W. Ahn, and C. Han, "Effects of Magnesium Chloride and Organic Additives on the Synthesis of Aragonite Precipitated Calcium Carbonate," *J. Cryst. Growth*, **310**, 2593–601 (2008).
[37]R. Beck and J. P. Andreassen, "The Onset of Spherulitic Growth in Crystallization of Calcium Carbonate," *J. Cryst. Growth*, **312**, 2226–38 (2010).
[38]K. K. Sand, J. D. Rodriguez-Blanco, E. Makovicky, L. G. Benning, and S. L. S. Stipp, "Crystallization of $CaCO_3$ in Water-Alcohol Mixtures: Spherulitic Growth, Polymorph Stabilization, and Morphology Change," *Cryst. Growth Des.*, **12**, 842–53 (2012).
[39]J. Jiang, J. Ye, G. Zhang, X. Gong, L. Nie, and J. Liu, "Polymorph and Morphology Control of $CaCO_3$ via Temperature and PEG During the Decomposition of $Ca(HCO_3)_2$," *J. Am. Ceram. Soc.*, **95**, 3735–8 (2012).
[40]F. Wang, Y. Guo, H. Wang, L. Yang, K. Wang, X. Ma, W. Yao, and H. Zhang, "Facile Preparation of Hydroxyapatite With a Three Dimensional Architecture and Potential Application in Water Treatment," *Cryst. Eng. Comm.*, **13**, 5634–7 (2011).
[41]M. Ni and B. D. Ratner, "Nacre Surface Transformation to Hydroxyapatite in a Phosphate Buffer Solution," *Biomaterials*, **24**, 4323–31 (2003).
[42]Y. Guo and Y. Zhou, "Transformation of Nacre Coatings Into Apatite Coatings in Phosphate Buffer Solution at Low Temperature," *J. Biomed. Mater. Res.*, **86A**, 510–21 (2008).
[43]Y. Shen, J. Zhu, H. Zhang, and F. Zhao, "*In Vitro* Osteogenetic Activity of Pearl," *Biomaterials*, **27**, 281–7 (2006).
[44]S. Kobayashi, M. Ui, H. Araikawa, T. Sakamoto, and K. Nakai, "Effect of Heat Treatments of Bioactive Nacre on HA Formation in SBF," *Mater. Sci. Forum*, **706–709**, 526–31 (2012).
[45]J. H. G. Rocha, A. F. Lemos, S. Agathapoulos, P. Valerio, S. Kannan, F. N. Oktar, and J. M. F. Ferreira, "Scaffolds for Bone Restoration From Cuttlefish," *Bone*, **37**, 850–7 (2005).
[46]A. Obata, D. Hasegawa, J. Nakamura, J. R. Jones, and T. Kasuga, "Induction of Hydroxycarbonate Apatite Formation on Polyethylene or Alumina Substrates by Spherical Vaterite Particles Deposition," *Mater. Sci. Eng., C*, **32**, 1976–81 (2012).
[47]H. Maeda, T. Kasuga, M. Nogami, Y. Hibino, K. I. Hata, M. Uada, and Y. Ota, "Biomimetic Apatite Formation on Poly(Lactic Acid) Composites Containing Calcium Carbonates," *J. Mater. Res.*, **17**, 727–30 (2002).
[48]T. Ikoma, T. Tonegawa, H. Watanaba, G. Chen, J. Tanaka, and Y. Mizushima, "Drug-Supported Microparticles of Calcium Carbonate Nanocrystals and Its Covering With Hydroxyapatite," *J. Nanosci. Nanotechno.*, **7**, 822–7 (2007).
[49]Y. Abe, T. Kokubo, and T. Yamamuro, "Apatite Coating on Ceramics, Metals and Polymers Using a Biomimetic Process," *J. Mater. Sci. Mat. Med.*, **1**, 233–8 (1990).
[50]T. Kokubo and H. Takadama, "How Useful is SBF in Predicting *In Vivo* Bone Bioactivity," *Biomaterials*, **27**, 2907–15 (2006).
[51]H. Sigel, K. H. Scheller, and B. Prijs, "Metal ion/Buffer Interactions. Stability of Alkali and Alkaline Earth Ion Complexes With Triethanolamine (Tea), 2-Amino-2(Hydroxymethyl)-1,3-Propanediol (Tris) and 2-[Bis(2-Hydroxyethyl)-Amino]2(Hydroxymethyl)-1,3-Propanediol (Bistris) in Aqueous and Mixed Solvents," *Inorg. Chim. Acta.*, **66**, 147–55 (1982).
[52]P. A. A. P. Marques, A. P. Serro, B. J. Saramago, A. C. Fernandes, M. C. F. Magalhaes, and R. N. Correia, "Mineralisation of Two Calcium Phosphate Ceramics in Biological Model Fluids," *J. Mater. Chem.*, **13**, 1484–90 (2003).
[53]A. P. Serro and B. Saramago, "Influence of Sterilization on the Mineralization of Titanium Implants Induced by Incubation in Various Biological Model Fluids," *Biomaterials*, **24**, 4749–60 (2003).
[54]D. Rohanova, A. R. Boccaccini, D. M. Yunos, D. Horkavcova, I. Brezovska, and A. Helebrant, "Tris Buffer in Simulated Body Fluid Distorts the Assessment of Glass-Ceramic Scaffold Bioactivity," *Acta Biomater.*, **7**, 2623–30 (2011).
[55]T. F. Baskett, "Sydney Ringer and Lactated Ringer's Solution," *Resuscitation*, **58**, 5–7 (2003).
[56]F. A. Moore, "The Use of Lactated Ringer's in Shock Resuscitation: The Good, the Bad and the Ugly," *J. Trauma.*, **70**, S15–6 (2011).
[57]M. A. Miller, M. R. Kendall, M. J. Kain, P. R. Larson, A. S. Madden, and A. C. Tas, "Testing of Brushite ($CaHPO_4{\cdot}2H_2O$) in Synthetic Biomineralization Solutions and *In Situ* Crystallization of Brushite Micro-Granules," *J. Am. Ceram. Soc.*, **95**, 2178–88 (2012).
[58]A. Pasinli, M. Yuksel, E. Celik, S. Sener, and A. C. Tas, "A New Approach in Biomimetic Synthesis of Calcium Phosphate Coatings Using Lactic Acid-Na Lactate Buffered Body Fluid Solution," *Acta Biomater.*, **6**, 2282–8 (2010).
[59]D. Sordelet and M. Akinc, "Preparation of Spherical, Monosized Y_2O_3 Precursor Particles," *J. Colloid Interf. Sci.*, **122**, 47–59 (1988).
[60]D. Kralj, L. Brecevic, and J. Kontrec, "Vaterite Growth and Dissolution in Aqueous Solution III. Kinetics of Transformation," *J. Cryst. Growth*, **177**, 248–57 (1997).
[61]G. Nehrke and P. Van Cappellen, "Framboidal Vaterite Aggregates and Their Transformation Into Calcite: A Morphological Study," *J. Cryst. Growth*, **287**, 528–30 (2006).
[62]A. C. Tas, "Use of Vaterite and Calcite in Forming Calcium Phosphate Cement Scaffolds," *Ceram. Eng. Sci. Proc.*, **28**, 135–50 (2008).
[63]A. C. Tas, "Monodisperse $CaCO_3$ Microtablets Forming at 70°C in Prerefrigerated $CaCl_2$-Gelatin-Urea Solutions," *Int. J. Appl. Ceram. Technol.*, **6**, 53–9 (2009).
[64]A. C. Tas, "Vaterite Bioceramics: Monodisperse $CaCO_3$ Biconvex Micropills Forming at 70°C in Aqueous $CaCl_2$-Gelatin-Urea Solutions," *Ceram. Eng. Sci. Proc.*, **30**, 139–52 (2009).
[65]F. A. Andersen and D. Kralj, "Determination of the Composition of Calcite-Vaterite Mixtures by Infrared Spectrophotometry," *Appl. Spectrosc.*, **45**, 1748–51 (1991).
[66]F. A. Andersen and L. Brecevic, "Infrared Spectra of Amorphous and Crystalline Calcium Carbonate," *Acta Chem. Scand.*, **45**, 1018–24 (1991).
[67]N. Koga and K. Nishikawa, "Mutual Relationship Between Solid-State Aragonite-Calcite Transformation and Thermal Dehydration of Included Water in Coral Aragonite," *Cryst. Growth Des.*, **14**, 879–87 (2014).
[68]R. de Ruiter, R. W. Tjerkstra, M. H. G. Duits, and F. Mugele, "Influence of Cationic Composition and pH on the Formation of Metal Stearates at Oil-Water Interfaces," *Langmuir*, **27**, 8738–47 (2011).
[69]S. Kim and C. B. Park, "Mussel-Inspired Transformation of $CaCO_3$ to Bone Minerals," *Biomaterials*, **31**, 6628–34 (2010).
[70]B. N. Bachra, O. R. Trautz, and S. L. Simon, "Precipitation of Calcium Carbonates and Phosphates. III. The Effect of Magnesium and Fluoride Ions on the Spontaneous Precipitation of Calcium Carbonates and Phosphates," *Arch. Oral Biol.*, **10**, 731–8 (1965).
[71]J. D. Termine and E. D. Eanes, "Calcium Phosphate Deposition From Balanced Salt Solutions," *Calc. Tiss. Res.*, **15**, 81–4 (1974).
[72]J. Y. Uan, J. K. Lin, Y. S. Sun, W. E. Yang, L. K. Chen, and H. H. Huang, "Surface Coatings for Improving the Corrosion Resistance and Cell Adhesion of AZ91D Magnesium Alloy Through Environmentally Clean Methods," *Thin Solid Films*, **518**, 7563–7 (2010).
[73]X. Cheng, P. L. Varona, M. J. Olszta, and L. B. Gower, "Biomimetic Synthesis of Calcite Films by a Polymer-Induced Liquid-Precursor (PILP) Process 1. Influence and Incorporation of Magnesium," *J. Cryst. Growth*, **307**, 395–404 (2007).
[74]J. J. M. Lenders, A. Dey, P. H. H. Bomans, J. Spielmann, M. M. R. M. Hendrix, G. de With, F. C. Meldrum, S. Harder, and N. A. J. M. Sommerdijk, "High Magnesium-Calcite Mesocrystals: A Coordination Chemistry Approach," *J. Am. Chem. Soc.*, **134**, 1367–73 (2012).
[75]K. J. Davis, P. M. Dove, and J. J. De Yoreo, "The Role of Mg^{2+} as an Impurity in Calcite Growth," *Science*, **290**, 1134–7 (2000).
[76]A. Villegas-Jimenez, A. Mucci, and M. A. Whitehead, "Theoretical Insights Into the Hydrated (10.4) Calcite Surface: Structure, Energetics, and Bonding Relationships," *Langmuir*, **25**, 6813–24 (2009).
[77]N. H. de Leeuw and S. C. Parker, "Surface Structure and Morphology of Calcium Carbonate Polymorphs Calcite, Aragonite and Vaterite: An Atomistic Approach," *J. Phys. Chem. B*, **102**, 2914–22 (1998).
[78]C. N. Rochette, S. Rosenfeldt, A. Heiss, T. Narayanan, M. Ballauff, and W. A. Jahnen-Dechent, "A Shielding Topology Stabilizes the Early Stage Protein-Mineral Complexes of Fetuin-A and Calcium Phosphate: A Time-Resolved Small-Angle X-ray Study," *Chem. BioChem.*, **10**, 735–40 (2009).
[79]A. C. Tas, "Calcium Metal to Synthesize Amorphous or Cryptocrystalline Calcium Phosphates," *Mater. Sci. Eng., C*, **32**, 1097–106 (2012).
[80]A. C. Tas, "Synthesis of Amorphous Calcium Phosphate or Poorly Crystalline Calcium Phosphate Powders by Using Ca Metal"; US Patent Pending, 20130209377 A1; August 15, 2013.
[81]F. Monchau, A. Lefevre, M. Descamps, A. Belquin-Myrdycz, P. Laffargue, and H. F. Hildebrand, "In Vitro Studies of Human and Rat Osteoclast Activity on Hydroxyapatite, β-Tricalcium Phosphate, Calcium Carbonate," *Biomol. Eng.*, **19**, 143–52 (2002).
[82]D. Geblinger, L. Addadi, and B. Geiger, "Nano-Topography Sensing by Osteoclasts," *J. Cell Sci.*, **123**, 1503–10 (2010).
[83]D. Duplat, A. Chabadel, M. Gallet, S. Berland, L. Bedouet, M. Rousseau, S. Kamel, C. Milet, P. Jurdic, M. Brazier, and E. Lopez, "The In Vitro Osteoclastic Degradation of Nacre," *Biomaterials*, **28**, 2155–62 (2007).
[84]J. C. Fricain, R. Bareille, F. Ulysse, B. Dupuy, and J. Amedee, "Evaluation of Proliferation and Protein Expression of Human Bone Marrow Cells Cultured on Coral Crystallized in the Aragonite or Calcite Form," *J. Biomed. Mater. Res.*, **42**, 96–102 (1998).
[85]C. Silve, E. Lopez, B. Vidal, D. C. Smith, S. Camprasse, G. Camprasse, and G. Couly, "Nacre Initiates Biomineralization by Human Osteoblasts Maintained In Vitro," *Calcif. Tissue Int.*, **51**, 363–9 (1992).
[86]C. J. Damien, J. L. Ricci, P. Christel, H. Alexander, and J. L. Patat, "Formation of a Calcium Phosphate-Rich Layer on Absorbable Calcium Carbonate Bone Graft Substitutes," *Calcif. Tissue Int.*, **55**, 151–8 (1994).
[87]C. Muller-Mai, C. Voigt, S. R. De Almeida Reis, H. Herbst, and U. M. Gross, "Substitution of Natural Coral by Cortical Bone and Bone Marrow in the Rat Femur," *J. Mater. Sci. Mater. Med.*, **7**, 479–88 (1996).
[88]M. Richard, E. Aguado, M. Cottrel, and G. Daculsi, "Ultrastructural and Electron Diffraction of the Bone-Ceramic Interfacial Zone in Coral and Biphasic CaP Implants," *Calcif. Tissue Int.*, **62**, 437–42 (1998). □